



## Research article

## Revisiting Fisher-KPP model to interpret the spatial spreading of invasive cell population in biology

Gour Chandra Paul <sup>a,\*</sup>, Tauhida <sup>a</sup>, Dipankar Kumar <sup>b</sup><sup>a</sup> Department of Mathematics, University of Rajshahi, Rajshahi 6205, Bangladesh<sup>b</sup> Department of Mathematics, Bangabandhu Sheikh Mujibur Rahman Science and Technology University, Gopalganj 8100, Bangladesh

## HIGHLIGHTS

- Closed-form solutions are obtained for the Fisher-KPP equation through the Homotopy analysis method.
- The effect of the proliferation rate of the model of interest on the entire population is studied.
- The invasive cell or the invasive population decreases in short time with the minimum proliferation rate.
- The Homotopy analysis method is found superior over other analytical methods.

## ARTICLE INFO

## Keywords:

Homotopy analysis method  
Fisher-KPP equation  
Closed-form solution  
Region of convergence

## ABSTRACT

In this paper, the homotopy analysis method, a powerful analytical technique, is applied to obtain analytical solutions to the Fisher-KPP equation in studying the spatial spreading of invasive species in ecology and to extract the nature of the spatial spreading of invasive cell populations in biology. The effect of the proliferation rate of the model of interest on the entire population is studied. It is observed that the invasive cell or the invasive population is decreased within a short time with the minimum proliferation rate. The homotopy analysis method is found to be superior to other analytical methods, namely the Adomian decomposition method, the homotopy perturbation method, etc. because of containing an auxiliary parameter, which provides us with a convenient way to adjust and control the region of convergence of the series solution. Graphical representation of the approximate series solutions obtained by the homotopy analysis method, the Adomian decomposition method, and the Homotopy perturbation method is illustrated, which shows the superiority of the homotopy analysis method. The method is examined on several examples, which reveal the ingenuity and the effectiveness of the method of interest.

## 1. Introduction

It is well recognized that reaction-convection-diffusion equations play a vital role in many areas of biology, ecology, chemistry, physics, engineering, and mathematical physics [1]. Diverse phenomena, such as population genetics, cellular ecology, reaction chemistry, heat transfer, combustion, fluid dynamics, foam drainage, crystal growth, soil-moisture, neurology, synergy, etc. can be described mathematically by using reaction-diffusion equations (RDEs) [1]. The Fisher-Kolmogorov-Petrovsky-Piskunov (Fisher-KPP) equation, also known as Fisher Kolmogorov (F-K) equation, is one of the most usually used RDEs in explaining most of the phenomena occurring in the fields men-

tioned above [2, 3, 4]. As in ref. [5], in one space dimension, the F-K equation can be written as follows:

$$\frac{\partial u}{\partial t} = D \frac{\partial^2 u}{\partial x^2} + \alpha u \left( 1 - \frac{u}{K} \right). \quad (1)$$

Eq. (1) outlines the spatial and temporal evolution of a population of motile and proliferative individuals with density  $u(x, t)$  that depends on the space  $x \geq 0$  and the time  $t > 0$  [2, 6]. Individuals in the population migrate through a linear diffusion process with diffusivity  $D > 0$ , the proliferation rate  $\alpha > 0$ , and have a carrying capacity density  $K > 0$  [5]. Solutions of the Fisher-KPP model on a semi-infinite domain that evolve from initial conditions (ICs) with compact support lead to long-

\* Corresponding author.

E-mail address: [pcgour2001@yahoo.com](mailto:pcgour2001@yahoo.com) (G.C. Paul).<https://doi.org/10.1016/j.heliyon.2022.e10773>

Received 14 February 2022; Received in revised form 4 June 2022; Accepted 22 September 2022

time travelling waves that move with speed  $c_{min} = 2\sqrt{\alpha D}$  [5]. The model also gives rise to traveling wave solutions (TWSs) with  $c > c_{min}$  for ICs that decrease sufficiently slowly as  $x \rightarrow \infty$ , though for most practical applications, we are interested in TWSs that travel with the minimum wave speed since ICs with compact support are often more relevant [7, 8, 9]. A TWS  $u(x, t) = u(\xi = x - ct)$ , propagating with a speed  $c$ , is restricted to be positive and bounded [10]. Therefore, the boundary conditions (BCs) for the TWS of Eq. (1) are usually  $u(\xi \rightarrow -\infty) \rightarrow 1$ ,  $u(\xi \rightarrow \infty) \rightarrow 0$ . Additionally,  $0 \leq u(x, t) \leq 1$  and  $c > 0$  is the wave speed.

Fisher [2] first introduced the RDE (linear diffusion and nonlinear growth of a population) given by Eq. (1) as an ideal for the extension of a mutant gene with an advantageous selection intensity  $D$  and an advantageous density  $u$ . This equation is encountered in chemical kinetics [11] and population dynamics which includes problems, such as the nonlinear evolution of a population in a one-dimensional habitat, and neutron population in a nuclear reaction. Moreover, the same equation occurs in logistic population growth models [12], flame propagation, neurophysiology, autocatalytic chemical reactions, and branching Brownian motion processes.

The F-K model and its various extensions have been used to study a broad range of biological phenomena. In this regard, in this paper, the generalized Fisher's equation in the following form is considered [13]:

$$\frac{\partial u}{\partial t} = \frac{\partial^2 u}{\partial x^2} + \alpha u(1 - u^\beta), \quad (2)$$

where  $\beta$  is a positive constant.

The F-K model and its various extensions are used to simulate the spatial expansion of invasion cell populations in biology [7, 8, 11, 12, 14, 15, 16]. In ecology, the F-K model has been used to study the spatial spreading of invasive species [17, 18, 19]. Further, as in refs. [3, 5, 20], the F-K model supports TWSs that have been broadly cultivated using a range of mathematical techniques. Therefore, the equation of choice is of great interest from the mathematical point of view as well. These TWSs of the F-K model are frequently used to mimic biological invasion [9]. Interestingly, the constant speed travelling waves (TWs) play a significant role in a wide number of medical applications [7, 8], and their behavior can be observed and measured experimentally. However, in spite of the measureless interest in TWSs to the F-K model, there are various features of these solutions that are biologically dissatisfactory [21]. For example, the TWSs do not have compact support for  $-\infty < x < \infty$ . On the other hand, the classical TWSs of the F-K equation do not involve a well-defined front and the cell density remains positive for  $u(x, t) \rightarrow 0$  as  $x \rightarrow \infty$ . Further, any restricted IC with compact support will always contribute to effective colonization and population growth. Unfortunately, the F-K equation is studied insufficiently to extract TWSs, as it is a challenging and difficult task of searching for such solutions to that equation [22]. To extract the TWSs of the F-K equation, researchers have, so far, applied some approximate and analytical methods. These methods include the Adomian decomposition method (ADM) [10], the homotopy perturbation method (HPM) [13, 23], the variational iteration method (VIM), etc. [24]. It is to be mentioned at this juncture that the series solutions attained by the HPM and the ADM are often convergent in restricted regions [25]. But sometimes it is required to enlarge the regions of convergence (ROC). To solve this problem, Liao proposed a powerful method, the homotopy analysis method (HAM) [26] on the basis of a fundamental concept in differential geometry and topology. The HAM is a semi-analytic approach for obtaining series solutions to a wide range of nonlinear equations, such as algebraic equations, ordinary differential equations (ODEs), partial differential equations (PDEs), integro-differential equations (IDEs), differential-difference equations (DDEs), and their coupled equations. Homotopy is used to define the conjunction between any two several objects in mathematics that have identical characteristics in various appearances [27]. The HAM is different from other analytical techniques for many purposes and recently it has been applied in many research fields. Unlike perturbation approaches, the HAM is independent of large/small physical parameters and hence it is valid whether

or not a nonlinear problem has small/large physical parameters. More crucially, unlike other perturbation and classic non-perturbation approaches, the HAM gives a simple mechanism to assure the convergence of series solutions, and hence the HAM is valid even for severely nonlinear situations. The HAM is based on the construction of a homotopy wherein an auxiliary linear operator is chosen to construct the homotopy. It is to be noted here that an auxiliary parameter is used in this method to control the ROC of the approximate series solution. A series solution of differential or integral equations achieved by the HAM converges very quickly over other analytical methods, namely the HPM, the ADM, the artificial small parameter method, the  $\delta$ -expansion method, and the decomposition method [28], and hence it may reduce a significant amount of computational cost. Also, the HAM provides greater flexibility in choosing auxiliary linear operators and initial approximations and as a result, a complicated nonlinear problem is transferred into a vast number of simpler linear sub-problems.

The HAM has recently been indicated to be useful for obtaining analytical solutions for nonlinear frequency response equations. Further, the HAM is employed to solve linear and nonlinear stiff ODEs, the matrix Riccati differential equation, and the Genesio system [29]. Furthermore, the HAM has been effectively used in many nonlinear problems, namely viscous flows [30], heat transfer, nonlinear water waves and oscillations [31], entropy analysis [32], and so on. Recently, the HAM has been used to analyze the reverse flow reactor (RFR) model [33]. Also, heat transfer and the MHD flow of viscoelastic fluids over an exponentially stretching surface are analyzed by the HAM [34]. Thus, from the literature point of view, it is clear that no evidence has been found to solve the F-K equation with the application of the HAM. Therefore, this research aims to use the effective and powerful method, the HAM, to solve nonlinear Fisher's equation and to explain the solutions from ecological and biological points of view. For this purpose, we solve Eq. (2) for several cases using the HAM in studying the spatial spreading of invasive species in ecology, as well as in the study of the spatial spreading of invasive cell populations. Since the HAM provides us with a greater flexibility to choose the initial approximation and an auxiliary linear operator to solve any nonlinear problems even if the problem has a closed-form solution, the solutions of the F-K equation are possible taking into account more than one initial approximation, which can be found later. Furthermore, because this approach divides a complicated nonlinear problem into an unlimited number of simple linear sub-problems, thereby a complicated nonlinear problem can easily be solved that cannot be unraveled via the other analytical problems available in the literature. The facts mentioned above signify the reason behind choosing the HAM to solve Fisher's equation. To the best of the authors' knowledge, this paper investigates for the first time, the effectiveness and the applicability of the HAM on the Fisher's equation by describing the solutions in the case of spatial spreading of invasive species in ecology and in biology to extract the characteristic of an invading cell population. Also, it describes the contribution of the proliferation rate in the Fisher-KPP model.

The rest of the paper is structured in the following way: The basic concept of the HAM for solving nonlinear problems is presented in Section 2. Applications of the HAM for solving the Fisher-KPP equation are introduced in Section 3, and the discussion of the attained results is presented in Section 4. Finally, the conclusion based on the outcomes emanated from the study is placed in Section 5.

## 2. Basic concept of the HAM for solving nonlinear problems

In this section, the basic idea for solving a nonlinear differential equation (NDE) by the HAM is presented briefly. For this purpose, we consider an NDE in the following form:

$$\mathcal{N}[u(x, t)] = 0, \quad (3)$$

where  $\mathcal{N}$  is a nonlinear operator,  $u$  is an unknown function of the independent variables  $x$  and  $t$ . For simplicity, all the ICs or BCs are ignored.

Then the zero-order deformation equation following Liao [26, 31] can be set out as

$$(1 - q)L[\varphi(x, t; q) - u_0(x, t)] = H(x, t)qh\mathcal{N}[\varphi(x, t; q)], \tag{4}$$

where  $L$  is an auxiliary linear operator,  $H(x, t)$  denotes a non-zero auxiliary function,  $q \in [0, 1]$  is an embedding parameter,  $h \neq 0$  is a convergence-control parameter (CPP), and  $u_0(x, t)$  is an initial guess of  $u(x, t)$ . Clearly when the embedding parameter  $q$  equals 0 and 1, then Eq. (4) holds  $\varphi(x, t; 0) = u_0(x, t)$ ,  $\varphi(x, t; 1) = u(x, t)$ , respectively. Thus, as  $q$  increases from 0 to 1, then the solution  $u(x, t; q)$  varies from the initial guess  $u_0(x, t)$  to the exact solution  $u(x, t)$ . Liao [35] expanded  $\varphi(x, t; q)$  in a Taylor series as follows:

$$\varphi(x, t; q) = u_0(x, t) + \sum_{m=1}^{\infty} u_m(x, t)q^m, \tag{5}$$

where

$$u_m(x, t) = \frac{1}{m!} \frac{\partial^m}{\partial q^m} \{\varphi(x, t; q)\}_{q=0}.$$

The convergence of the series given by Eq. (5) depends upon the choice of the auxiliary linear operator, the initial guess, CCP  $h$ , and the auxiliary function. If they are chosen properly, then the series (5) converges at  $q = 1$ , we have the homotopy series solution as follows:

$$u(x, t) = u_0(x, t) + \sum_{m=1}^{\infty} u_m(x, t).$$

Differentiating  $m$ -times the zero-order deformation equation given by Eq. (4) with respect to  $q$  and dividing by  $m!$ , we can easily derive the  $m$ th-order deformation equation. Finally, setting  $q = 0$ , we have

$$L[u_m(x, t) - \chi_m u_{m-1}(x, t)] = H(x, t)hR_m(u_{m-1}(x, t)), \tag{6}$$

where  $R_m(u_{m-1}(x, t)) = \frac{1}{(m-1)!} \frac{\partial^{m-1}}{\partial q^{m-1}} \{\varphi(x, t; q)\}_{q=0}$  and  $\chi_m = \begin{cases} 0, & m \leq 1 \\ 1, & m > 1. \end{cases}$

In this fashion, the original nonlinear equation is converted into an infinite number of linear ones. It should be accentuated that the linear equations can easily be solved by any symbolic computation software, such as Maple, Mathematica, Matlab, and so on.

Applying  $L^{-1}$  on both sides of Eq. (6), we get

$$u_m(x, t) = \chi_m u_{m-1}(x, t) + H(x, t)hL^{-1}R_m(u_{m-1}(x, t)).$$

In this way, it is easy to obtain  $u_m$  ( $m \geq 1$ ), at  $m$ th-order, and thereby, we have

$$u(x, t) = \sum_{m=0}^M u_m(x, t). \tag{7}$$

When  $M \rightarrow \infty$ , an accurate approximation of Eq. (3) is obtained. If Eq. (3) has a unique solution, then this method will yield the unique solution and if Eq. (3) does not possess a unique solution, the HAM will yield a solution among many other possible solutions.

### 3. Applications of the HAM to Fisher's equation

In this section, we envisage the generalized Fisher's equation in the following form [13]:

$$\frac{\partial u}{\partial t} = \frac{\partial^2 u}{\partial x^2} + \alpha u(1 - u^\beta). \tag{8}$$

To incorporate our discussion, four important cases of nonlinearity, which correspond to some real physical processes, have been investigated to show the reliability of the proposed scheme. For this purpose, several ICs have been selected.

**Case 1:** In this case, we will solve Eq. (8) for  $\alpha = 1$  and  $\beta = 1$  (Fisher's equation), i.e., we will solve the following equation with the help of the HAM:

$$\frac{\partial u}{\partial t} = \frac{\partial^2 u}{\partial x^2} + u(1 - u). \tag{9}$$

Eq. (9) can be used to study flame propagation and nuclear reactors. To solve Eq. (9) by the HAM, at first, we need to choose an appropriate initial approximation. To illustrate our purposes, we consider the initial approximation of Eq. (9) following Singh et al. [13] as  $u(x, 0) = \gamma$ , where  $\gamma$  is an arbitrary constant. For the analytical solution of Eq. (9), we choose the linear operator as  $L\varphi(x; q) = \frac{\partial \varphi(x; q)}{\partial t}$  with the property  $L[c] = 0$ , where  $c$  is a constant and we assume that  $L^{-1}$  exists and is defined as  $L^{-1} = \int_0^t (\cdot) dt$ .

Now, we define the nonlinear operator  $\mathcal{N}$  as

$$\mathcal{N}[\varphi(x; q)] = \frac{\partial u(x; q)}{\partial t} - \frac{\partial^2 u(x; q)}{\partial x^2} + u(x; q)[1 - u(x; q)]. \tag{10}$$

Using the definition given by Eq. (4), we construct the zero-order deformation equation as follows:

$$(1 - q)L[\varphi(x, t; q) - u_0(x, t)] = H(x, t)qh\mathcal{N}[\varphi(x, t; q)]. \tag{11}$$

For  $q = 0$  and  $q = 1$ , from Eq. (11), we can write

$$\varphi(x, t; 0) = u_0(x, t) \text{ and } \varphi(x, t; 1) = u(x, t), \text{ respectively.}$$

Thus, the deformation equation of the  $m$ th order is attained as

$$L[u_m(x, t) - \chi_m u_{m-1}(x, t)] = H(x, t)hR_m(u_{m-1}(x, t)). \tag{12}$$

Therefore, the solution of the  $m$ th order deformation equation by taking  $L^{-1}$  on both sides of Eq. (12) can be presented as

$$u_m(x, t) = \chi_m u_{m-1}(x, t) + H(x, t)hL^{-1}R_m(u_{m-1}(x, t)). \tag{13}$$

For  $m \geq 1$  and  $H(x, t) = 1$ , using Eq. (10), we obtain

$$R_m(u_{m-1}(x, t)) = \frac{\partial u_{m-1}(x, t)}{\partial t} - \frac{\partial^2 u_{m-1}(x, t)}{\partial x^2} - u_{m-1}(x, t) + \sum_{i=0}^{m-1} u_i(x, t)u_{m-1-i}(x, t). \tag{14}$$

Hence, from Eq. (14), we get

$$R_1(u_0) = \frac{\partial u_0(x, t)}{\partial t} - \frac{\partial^2 u_0(x, t)}{\partial x^2} - u_0(x, t) + (u_0(x, t))^2, \\ R_2(u_1) = \frac{\partial u_1(x, t)}{\partial t} - \frac{\partial^2 u_1(x, t)}{\partial x^2} - u_1(x, t) + 2u_0(x, t)u_1(x, t), \dots$$

Substituting  $R_m(u_{m-1}(x, t))$  in Eq. (13) and solving for  $u_m(x, t)$ , we see

$$u_1(x, t) = hL^{-1}R_1(u_0(x)) = h\gamma t(\gamma - 1), \\ u_2(x, t) = u_1(x, t) + hL^{-1}R_2(u_1(x)) = \frac{1}{2}h\gamma t(\gamma - 1)(2h\gamma t - ht + 2h + 2), \dots$$

Hence, the approximate solution of Eq. (9) by the HAM is given by (see Eq. (7))

$$u(x, t) = \sum_{m=0}^M u_m(x, t) \\ = u_0(x, t) + u_1(x, t) + u_2(x, t) + \dots \\ = \gamma + h\gamma t(\gamma - 1) + \frac{1}{2}h\gamma t(\gamma - 1)(2h\gamma t - ht + 2h + 2) + \dots \tag{15}$$

When  $h \rightarrow -1$ , then we attain the exact solution  $u(x, t)$  from Eq. (15), which can be presented in the following form:

$$u(x, t) = \gamma + \gamma(1 - \gamma)t + \frac{\gamma(1 - \gamma)(1 - 2\gamma)t^2}{2!} + \gamma(1 - \gamma)(1 - 6\gamma + 6\gamma^2)\frac{t^3}{3!} + \dots \tag{16}$$

By using any symbolic computation system and performing some algebraic operations, the solution given by Eq. (16) can be brought to the following closed-form solution:

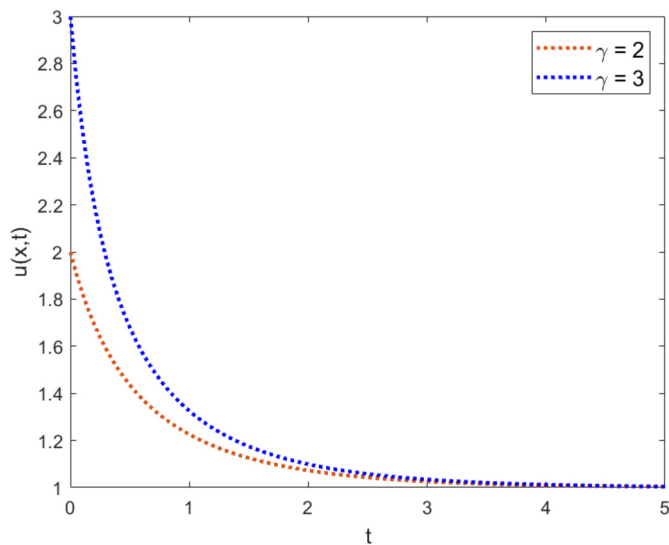


Fig. 1. 2D plot of the solution of Eq. (9) given by Eq. (17) with  $\gamma = 2$  and  $\gamma = 3$ .

$$u(x, t) = \frac{\gamma e^t}{1 - \gamma + \gamma e^t}, \tag{17}$$

which is the exact solution to the problem specified by Eq. (9).

From the initial solution and the obtained solution, it is perceived that the initial solution can be generated from the closed-form solution by setting  $t = 0$ .

The two-dimensional (2D) graphical illustration of the solution of Eq. (9) given by Eq. (17) for some values of the ICs is presented in Fig. 1 for a better perspective. It is perceived from the figure that if  $t$  increases from 0 to 5, then  $u(x, t)$  decreases for all values of  $x$  with the ICs  $\gamma = 2, \gamma = 3$ . The solution given by Eq. (17) achieved via the HAM is exactly the same with those acquired by the ADM [10], the HPM [13, 23], and the VIM [24], which is the exact solution of Eq. (9) with the specified initial approximation.

**Case 2:** In this case, we solve Eq. (9) with another initial approximation to examine the flexibility of the HAM in the case of choosing several initial approximations. It is pertinent to note here that the HAM has greater flexibility in choosing an initial approximation, i.e., we can choose several approximations. For suitability and to make sense clear, we choose another initial solution of Eq. (9) following Hasnain and Saqib [36] as

$$u(x, 0) = \left(1 + e^{\frac{1}{\sqrt{6}}x}\right)^{-2}. \tag{18}$$

By the same process detailed in Case 1, we obtain

$$u_1(x, t) = -\frac{5}{3} \frac{he^{\frac{1}{\sqrt{6}}x} t}{\left(1 + e^{\frac{1}{\sqrt{6}}x}\right)^3},$$

$$u_2(x, t) = \frac{5}{36} \frac{he^{\frac{1}{\sqrt{6}}x} t \left(10he^{\frac{1}{\sqrt{6}}x} t - 12he^{\frac{1}{\sqrt{6}}x} - 5ht - 12he^{\frac{1}{\sqrt{6}}x} - 12h - 12\right)}{\left(1 + e^{\frac{1}{\sqrt{6}}x}\right)^4}, \dots$$

Hence, the approximate solution of Eq. (9) by the HAM can be set as

$$u(x, t) = \sum_{m=0}^M u_m(x, t)$$

$$= u_0(x, t) + u_1(x, t) + u_2(x, t) + \dots$$

$$= \frac{1}{\left(1 + e^{\frac{1}{\sqrt{6}}x}\right)^2} - \frac{5}{3} \frac{he^{\frac{1}{\sqrt{6}}x} t}{\left(1 + e^{\frac{1}{\sqrt{6}}x}\right)^3}$$

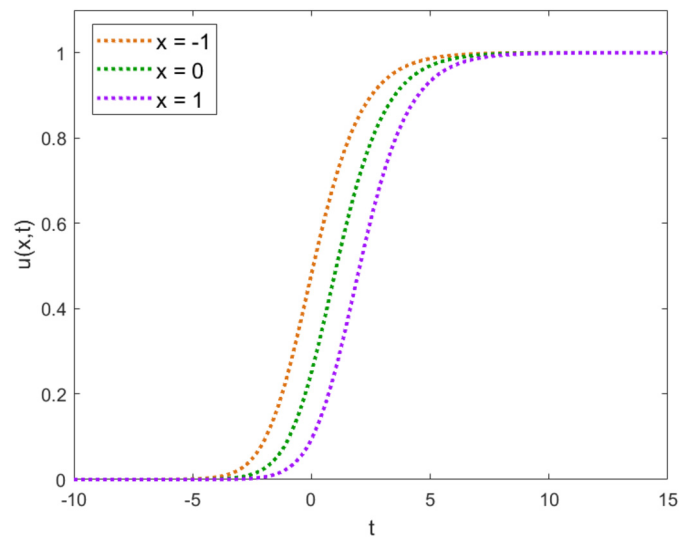


Fig. 2. 2D plot of the solution given by (21) of Eq. (9) for  $x = -1, x = 0,$  and  $x = 1$ .

$$+ \frac{5}{36} \frac{he^{\frac{1}{\sqrt{6}}x} t \left(10he^{\frac{1}{\sqrt{6}}x} t - 12he^{\frac{1}{\sqrt{6}}x} - 5ht - 12he^{\frac{1}{\sqrt{6}}x} - 12h - 12\right)}{\left(1 + e^{\frac{1}{\sqrt{6}}x}\right)^4} + \dots \tag{19}$$

Thus, the exact solution,  $u(x, t)$  obtained from Eq. (19) as  $h \rightarrow -1$  is given by

$$u(x, t) = \frac{1}{\left(1 + e^{\frac{1}{\sqrt{6}}x}\right)^2} + \frac{5}{3} \frac{e^{\frac{1}{\sqrt{6}}x} t}{\left(1 + e^{\frac{1}{\sqrt{6}}x}\right)^3} + \frac{5}{36} \frac{e^{\frac{1}{\sqrt{6}}x} t \left(10e^{\frac{1}{\sqrt{6}}x} t - 5t\right)}{\left(1 + e^{\frac{1}{\sqrt{6}}x}\right)^4} + \dots \tag{20}$$

By performing some algebraic operations with the aid of a symbolic computation software, the above solution presented in Eq. (20) can be brought to the following closed-form solution:

$$u(x, t) = \left(1 + e^{\frac{1}{\sqrt{6}}x - \frac{5}{6}t}\right)^{-2}. \tag{21}$$

The solution given by Eq. (21) is another exact solution to the problem given by Eq. (9). It is obvious that the initial approximation given by Eq. (18) can be procured from the obtained solution by setting  $t = 0$ . For interpreting the result physically, its 2D graphical illustration is presented in Fig. 2.

Fig. 2 is presented with  $\alpha = 1, \beta = 1,$  and initial approximation  $u(x, 0) = \left(1 + e^{\frac{1}{\sqrt{6}}x}\right)^{-2}$  for varying  $x \in [-1, 1]$  where  $t$  varies from  $-10$  to  $15$ . It is perceived from Fig. 2 that  $u(x, t)$  increases over time, and after some time ( $t > 5$ ),  $u(x, t)$  turns out to be constant.

**Case 3:** In this case, we examine the Fisher's equation given by Eq. (8) for proliferation rate  $\alpha = 6$  whereas  $\beta = 1$  (Fisher's equation), i.e., we will seek the solution of the following equation:

$$\frac{\partial u}{\partial t} = \frac{\partial^2 u}{\partial x^2} + 6u(1 - u). \tag{22}$$

In order to solve Eq. (22) by the HAM and illustrate our purpose, first, as in ref. [13], we consider the initial approximation of Eq. (22) as

$$u(x, 0) = \frac{1}{(1 + e^x)^2}. \tag{23}$$

According to the solution procedure detailed in case 1, the nonlinear operator is defined as

$$\mathcal{N}[\varphi(x; q)] = \frac{\partial u(x; q)}{\partial t} - \frac{\partial^2 u(x; q)}{\partial x^2} + 6u(x; q)[1 - u(x; q)], \tag{24}$$

and then the solution of the deformation equation of the  $m$ th order is given by

$$u_m(x, t) = \chi_m u_{m-1}(x, t) + H(x, t) h L^{-1} R_m(u_{m-1}(x, t)), \tag{25}$$

where  $H(x, t) = 1$  and

$$R_m(u_{m-1}(x, t)) = \frac{\partial u_{m-1}(x, t)}{\partial t} - \frac{\partial^2 u_{m-1}(x, t)}{\partial x^2} - 6u_{m-1}(x, t) + 6 \sum_{i=0}^{m-1} u_i(x, t) u_{m-1-i}(x, t). \tag{26}$$

Hence, from Eqs. (24) and (26), we attain

$$R_1(u_0) = \frac{\partial u_0(x, t)}{\partial t} - \frac{\partial^2 u_0(x, t)}{\partial x^2} - 6u_0(x, t) + 6(u_0(x, t))^2, \\ R_2(u_1) = \frac{\partial u_1(x, t)}{\partial t} - \frac{\partial^2 u_1(x, t)}{\partial x^2} - 6u_1(x, t) + 12u_0(x, t)u_1(x, t), \dots$$

Substituting  $R_m(u_{m-1}(x, t))$  in Eq. (25) and solving for  $u_m(x, t)$ , it is easy to see

$$u_1(x, t) = h L^{-1} R_1(u_0(x)) = -\frac{10ht e^x t}{(1 + e^x)^3}, \\ u_2(x, t) = u_1(x, t) + h L^{-1} R_2(u_1(x)) \\ = \frac{5he^x t (10he^x t - 2he^x - 5ht - 2e^x - 2h - 2)}{(1 + e^x)^4}, \\ \dots \dots \dots$$

Hence, the series solution of Eq. (22) attained by the HAM is given by

$$u(x, t) = \sum_{m=0}^M u_m(x, t) = u_0(x, t) + u_1(x, t) + u_2(x, t) + \dots \tag{27}$$

The exact solution  $u(x, t)$  obtained from Eq. (27) as  $h \rightarrow -1$  is given by

$$u(x, t) = \frac{1}{(1 + e^x)^2} + \frac{10te^x t}{(1 + e^x)^3} + \frac{25e^x (2e^x - 1)t^2}{(1 + e^x)^4} + \dots \tag{28}$$

With some algebraic operations performed by a symbolic computational tool, it is easy to see the solution presented by Eq. (28) in the following closed-form:

$$u(x, t) = \frac{1}{(1 + e^{x-5t})^2}, \tag{29}$$

which is the exact solution of Eq. (22) for case 3. It is noticeable that the initial solution given by Eq. (23) can be produced from Eq. (29) by setting  $t = 0$ .

The 2D plot of the solution of Eq. (22) given by Eq. (29) is displayed in Fig. 3 for a clear understanding.

Fig. 3 is presented with  $\alpha = 6$ ,  $\beta = 1$ , and  $u(x, 0) = \frac{1}{(1+e^x)^2}$ , for varying  $x \in [-1, 1]$ , where  $t$  varies from  $-3$  to  $3$ . It is perceived from Fig. 3 that  $u(x, t)$  increases over time and after some time,  $u(x, t)$  becomes constant. The closed-form solution of Eq. (22) given by Eq. (29) is found to be exactly the same with those extracted via the ADM [10], the HPM [13, 23], and the VIM [24], which is the exact solution of Eq. (22) with the given initial approximate solution.

**Case 4:** In this case, we examine the Fisher-KPP equation specified by Eq. (8) for  $\alpha = 1$  and  $\beta = 6$  (generalized Fisher's equation) i.e., we seek out the solution of the equation appended below:

$$\frac{\partial u}{\partial t} = \frac{\partial^2 u}{\partial x^2} + u(1 - u^6). \tag{30}$$

The equation has applications in biology, especially in tumor growth and invasion. To solve Eq. (30) by the HAM and point out our intention, we consider the initial approximation following Singh et al. [13] as

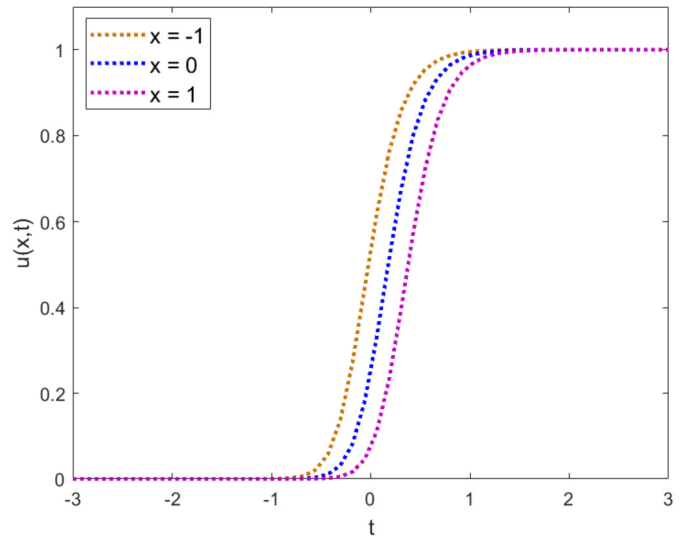


Fig. 3. 2D plot of the solution of Eq. (22) given by (29) with  $x = -1$ ,  $x = 0$ , and  $x = 1$ .

$$u(x, 0) = \left(1 + e^{\frac{3}{2}x}\right)^{-\frac{1}{3}}. \tag{31}$$

On the basis of the process detailed in obtaining the solution in case 1, the nonlinear operator can be defined as

$$\mathcal{N}[\varphi(x; q)] = \frac{\partial u(x; q)}{\partial t} - \frac{\partial^2 u(x; q)}{\partial x^2} + u(x; q)[1 - u^6(x; q)], \tag{32}$$

and then the solution of the deformation equation of the  $m$ th order leads to

$$u_m(x, t) = \chi_m u_{m-1}(x, t) + H(x, t) h L^{-1} R_m(u_{m-1}(x, t)). \tag{33}$$

Then from Eqs. (32) and (33) maintaining the same procedure detailed above, we attain the following results:

$$R_1(u_0) = \frac{\partial u_0(x, t)}{\partial t} - \frac{\partial^2 u_0(x, t)}{\partial x^2} - u_0(x, t) + (u_0(x, t))^7, \\ R_2(u_1) = \frac{\partial u_1(x, t)}{\partial t} - \frac{\partial^2 u_1(x, t)}{\partial x^2} - u_1(x, t) + 7(u_0(x, t))^6 u_1(x, t), \\ R_3(u_2) = \frac{\partial u_2(x, t)}{\partial t} - \frac{\partial^2 u_2(x, t)}{\partial x^2} - u_2(x, t) + 7u_2(x, t)(u_0(x, t))^6 \\ + 21(u_2(x, t))^2(u_0(x, t))^5, \dots$$

Substituting  $R_m(u_{m-1}(x, t))$  in Eq. (33) and solving for  $u_m(x, t)$ , we get

$$u_1(x, t) = h L^{-1} R_1(u_0(x)) = -\frac{5}{4} \frac{hte^{\frac{3}{2}x}}{\left(1 + e^{\frac{3}{2}x}\right)^{\frac{4}{3}}}, \\ u_2(x, t) = u_1(x, t) + h L^{-1} R_2(u_1(x)), \\ = \frac{5}{32} \frac{hte^{\frac{3}{2}x} \left(5hte^{\frac{3}{2}x} - 8 - 8e^{\frac{3}{2}x} - 8hte^{\frac{3}{2}x} - 15ht - 8h\right)}{\left(1 + e^{\frac{3}{2}x}\right)^{\frac{7}{3}}}, \text{ and so on.}$$

By the same process, we can attain the terms, as desirable, of the series. Hence, the approximate series solution of Eq. (30) by the HAM is given by

$$u(x, t) = \sum_{m=0}^M u_m(x, t) = u_0(x, t) + u_1(x, t) + u_2(x, t) + \dots \tag{34}$$

When  $h \rightarrow -1$ , then we can put forward  $u(x, t)$  given by Eq. (34) in the following form:

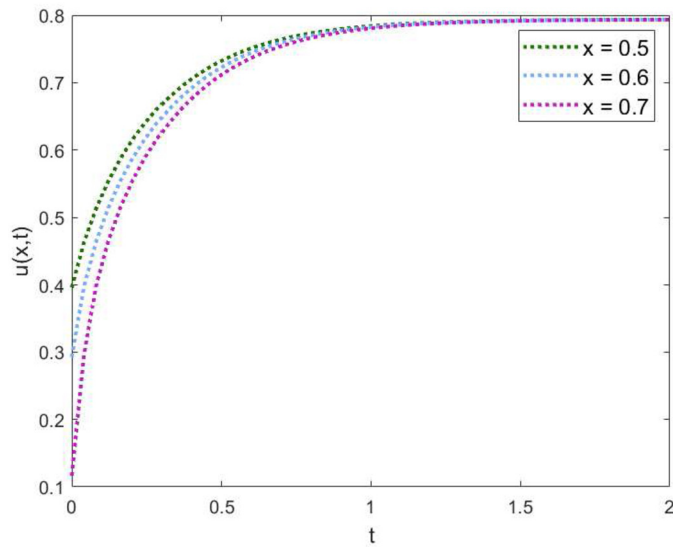


Fig. 4. 2D plot of the solution of Eq. (30) given by Eq. (36) with  $x = 0.5$ ,  $x = 0.6$ , and  $x = 0.7$ .

$$u(x, t) = \frac{1}{\left(1 + e^{\frac{3}{2}x}\right)^{\frac{1}{3}}} + \frac{5}{4} \frac{e^{\frac{3}{2}x}}{\left(1 + e^{\frac{3}{2}x}\right)^{\frac{4}{3}}} t + \frac{25}{32} \frac{e^{\frac{3}{2}x} \left(e^{\frac{3}{2}x} - 3\right)}{\left(1 + e^{\frac{3}{2}x}\right)^{\frac{7}{3}}} \frac{t^2}{2!} + \dots \quad (35)$$

By performing some algebraic operations through any symbolic computation software, one can see  $u(x, t)$  given by Eq. (35) in the following closed-form:

$$u(x, t) = \left\{ \frac{1}{2} \tanh \left( -\frac{3}{4} \left( x - \frac{5}{2} t \right) + \frac{1}{2} \right) \right\}^{\frac{1}{3}}, \quad (36)$$

which is the exact solution of Eq. (30). It is obvious that the initial solution given by Eq. (31) can be produced from Eq. (36) by setting  $t = 0$ .

The solution of Eq. (30) given by Eq. (36) is displayed in Fig. 4 for comprehending the intricate physical interpretation. Fig. 4 is presented with  $\alpha = 1$ ,  $\beta = 6$ , and  $u(x, 0) = \left(1 + e^{\frac{3}{2}x}\right)^{-\frac{1}{3}}$ , where  $t$  varies from 0 to 2. It is perceived from Fig. 4 that  $u(x, t)$  increases initially and after some time,  $u(x, t)$  turns out to be constant for all values of  $x$ . The closed-form solution of Eq. (30) achieved through the HAM given by Eq. (36) provides the same results as those picked up via the ADM [10], the HPM [13, 23], and the VIM [24], which is the exact solution of Eq. (30) with the given initial approximate solution.

**Theorem** (Convergence analysis [37, 38, 39, 40]). Assume that  $u_0, u_1, u_2, \dots$  are derived by the procedure mentioned above. Then, the series  $u(x, t) = u_0(x, t) + \sum_{m=0}^{\infty} u_m(x, t)$  converges if there exists  $0 < r < 1$  such that  $\|u_{m+1}\| \leq r \|u_m\|$  for all  $m \geq m_0$  and for some  $m_0 \in \mathbb{N}$ , the set of natural numbers.

Furthermore, the estimated error can be given as  $\|u - \sum_{m=0}^k u_m(x, t)\| \leq \frac{r^{k+1}}{1-r} \|u_0\|$ .

#### 4. Discussion of the attained results

In this section, we describe the effectiveness and the applicability of the HAM to analyze the solution of the Fisher’s equation with the viewpoint of the spatial spreading of invasive species in ecology and in biology, the disposition of the spatial spreading of invasive cell populations, and the influence of the proliferation rate.

If we consider the Fisher-KPP model in the case of spatial spreading of invasive species in ecology or to extract the nature of the spatial

spreading of invasive cell populations in biology, Figs. 1–4 may be described as follows: It is clear from Fig. 1 obtained for the proliferation rate  $\alpha = 1$  that at the initial time  $t$ , the invasive species are located to a critical level, but as time  $t$  increases, the invasive species or the invasive cell populations decrease continuously with constant shape and constant speed, and after a brief period of time, the invasion is found to be constant. Thus, in this case, Fisher’s equation does not allow the invasive species or the invasive cell populations to go extinct.

With the same proliferation rate, we solve Eq. (9) in case 2 with the initial approximation  $u(x, 0) = \left(1 + e^{\frac{1}{\sqrt{6}}x}\right)^{-2}$ , and this is possible, because the HAM provides us with a proper base function so as to yield a better approximation of the nonlinear problem. It is seen from Fig. 2 that if the invasion species stand before starting time of our investigation, then the invasion increases over time, but after a while, the invasion becomes constant. This case also does not allow the solution to go extinct.

But for the same proliferation rate, it is seen from Fig. 4 for the initial approximation  $u(x, 0) = \left(1 + e^{\frac{3}{2}x}\right)^{-\frac{1}{3}}$  that if some species are invasion, then the invasion increases when time increases and after a brief period of time, the invasion remains constant. Thus, the solution of Eq. (30) given by Eq. (36) does not allow the invasive species or the invasive cell populations to go extinct.

Finally, if we increase the proliferation rate, then Fig. 3 illustrated for the solution given by Eq. (29) of Eq. (22) for the initial approximation  $u(x, 0) = \frac{1}{(1+e^x)^2}$  presents that if the invasion species stand before starting our investigation time, then it is easily perceived from the figure (Fig. 3) that the invasion increases over time, but after a few times, the invasion becomes constant. This case also does not allow the solution to go extinct. Thus, from the above four cases, we notice that Fisher’s equation gives the solution with compact support, but it does not allow the solution to go extinct. Furthermore, in the long-time limit, the solutions of Fisher’s equation lead to a constant speed and constant shape TW. It is of interest to note here that for every positive IC with compact support, Fisher’s equation will always amplify to a TW that moves with a minimum speed.

It can easily be perceived from the above results that the general solution of the Fisher’s equation  $\frac{\partial u}{\partial t} = \frac{\partial^2 u}{\partial x^2} + \alpha u(1 - u)$  is given by

$$u(x, t) = \left( 1 + e^{\sqrt{\frac{\alpha}{6}} \left( x - \frac{5}{6} \alpha t \right)} \right)^{-2}. \quad (37)$$

From the solution given by Eq. (37), we notice that the proliferation rate  $\alpha$  is the only parameter used to describe the entire population. To examine the effect of  $\alpha$ , the graphical illustration of the solution given by Eq. (37) for some values of  $\alpha$  is presented in Fig. 5 for a better perspective. It is perceived from Fig. 5 that a TW is approached that travels in the positive  $x$ -direction with constant shape and constant speed in the case of spatial spreading of invasive species in ecology or the spatial spreading of invasive cell populations in biology. The invasive cell population propagates severally on a semi-infinite region due to the variation of proliferation rate (see Fig. 5). For the proliferation rate  $\alpha = 1$ , Fig. 5(a) indicates that the invasion starts to decay in space quickly with a constant speed and after a short spatial distance, the invasion is found to be constant. For the proliferation rate  $\alpha = 2$ , Fig. 5(b) shows that for  $t = 0$ , the invasion decreases quickly in space that means the propagation of the invasion is very less. On the other hand, for other times, at first, the invasion spreads out over space and then begins to decay as the spatial distance increases, and the invasion becomes constant. Finally, Fig. 5(c)–(d) shows that the invasion declines after overlong spatial distance which signifies that the rate of the spatial spreading is maximum in those cases. It is clarified from the figure that the rate of invasion is almost stationary, but it does not go extinct. Therefore, it is perceived from the figure that the invasion

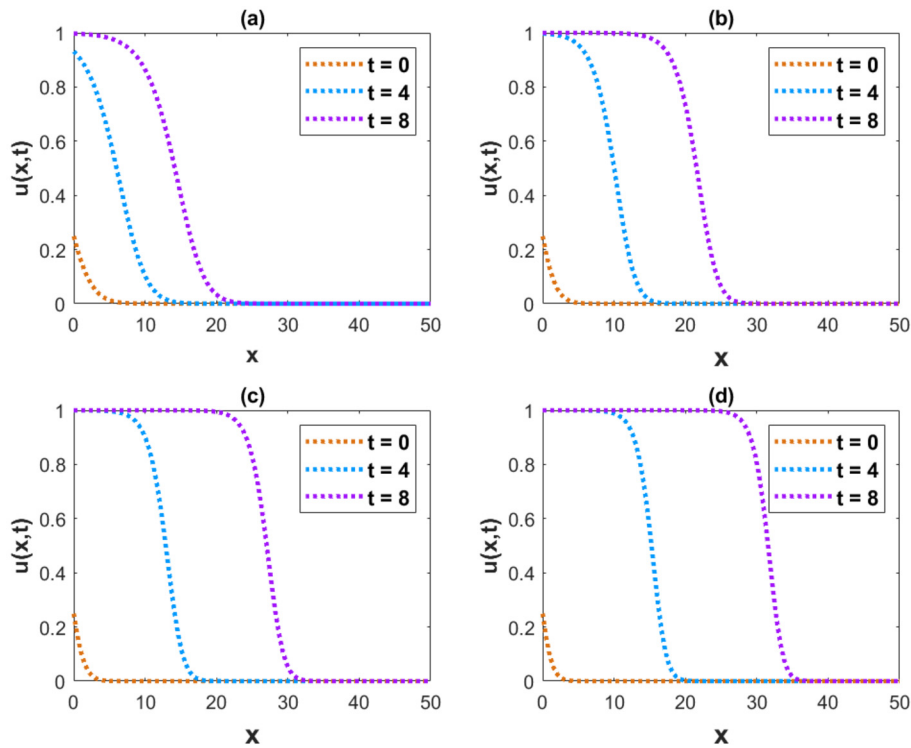


Fig. 5. 2D plot of the solution given by Eq. (37) for (a)  $\alpha = 1$ , (b)  $\alpha = 2$ , (c)  $\alpha = 3$ , and (d)  $\alpha = 4$ .

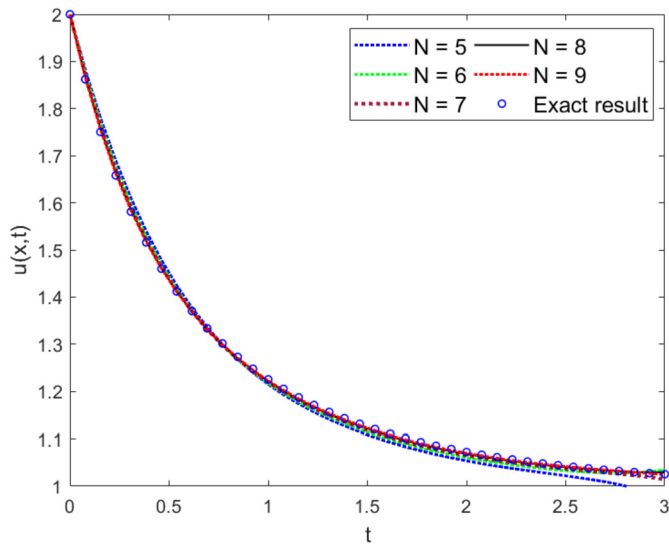


Fig. 6. Graphical illustration of the approximate series solution given by Eq. (15) with several orders of Eq. (9) and its exact solution.

spread out over space quickly when the proliferation rate is increased which means that the invasion starts to decrease rapidly only when the proliferation rate is lowered.

Further, it can be perceived from Fig. 5 that the solution approaches a travelling wave that moves in the positive  $x$ -direction with constant speed and constant shape. Our solutions confirm that the speed of propagation is minimum, as expected.

To examine the convergence of the series given by Eq. (15), we present graphically the HAM approximation solutions with several orders of Eq. (9) taking  $h = -0.28$ ,  $\gamma = 2$  and its exact solution in Fig. 6. It can be observed from Fig. 6 that the HAM solution converges to the exact solution after only 5 terms. We have also estimated the root mean square error (RMSE) between our approximate results taking the first

Table 1. The AErr of the approximate series solution (given by Eq. (15)) of Eq. (9) and its exact solution.

$t$	AErr with $\gamma = 2, h = -0.28$				
	$N = 5$	$N = 6$	$N = 7$	$N = 8$	$N = 9$
0	0	0	0	0	0
0.50	$1.52 \times 10^{-2}$	$6.45 \times 10^{-3}$	$2.33 \times 10^{-3}$	$4.90 \times 10^{-4}$	$2.55 \times 10^{-4}$
1.00	$1.05 \times 10^{-2}$	$8.35 \times 10^{-3}$	$6.12 \times 10^{-3}$	$4.33 \times 10^{-3}$	$3.02 \times 10^{-3}$
1.50	$1.71 \times 10^{-2}$	$1.15 \times 10^{-2}$	$7.64 \times 10^{-3}$	$5.02 \times 10^{-3}$	$3.27 \times 10^{-3}$
2.00	$1.88 \times 10^{-2}$	$1.19 \times 10^{-2}$	$7.38 \times 10^{-3}$	$4.42 \times 10^{-3}$	$2.54 \times 10^{-3}$
2.50	$2.06 \times 10^{-2}$	$9.87 \times 10^{-3}$	$5.87 \times 10^{-3}$	$2.67 \times 10^{-3}$	$1.03 \times 10^{-3}$
3.00	$4.95 \times 10^{-2}$	$2.03 \times 10^{-2}$	$1.09 \times 10^{-2}$	$3.79 \times 10^{-3}$	$9.56 \times 10^{-4}$

8 terms and the exact result. The estimated RMSE value is found to be  $4.7648 \times 10^{-4}$ , which is reasonable. To ensure the proper judgement of the above statements, the absolute error (AErr) between the approximate series solution given by Eq. (15) with several orders of Eq. (9) and its exact solution is presented in Table 1 taking  $\gamma = 2$  and  $h = -0.28$ . From Table 1, it is revealed that the AErr is minimum at the highest order approximated solution. That means the HAM approximated series solution converges to the exact solution when  $N$  tends to infinity.

To test the superiority of the HAM over the ADM and the HPM, we present graphically the exact solution of Eq. (9) and its approximate series solutions taking the first 8 terms attained by the HAM, the ADM, and the HPM in Fig. 7. It is to be noted here that the approximate series solutions of Eq. (9) by the ADM and the HPM are achieved by taking  $h = -1$  in Eq. (15), which is the same as the ones produced by the ADM [10] and the HPM [13, 23]. Therefore, the series solution attained by the HAM is superior to the series solutions that came out through the ADM and the HPM. It is seen also from Fig. 7 that the HAM result achieved by taking  $h = -0.55$  converges rapidly to the exact solution than the ADM and the HPM. To clarify the above judgment, the AErrs between the approximate series solution (15) of Eq. (9) obtained by the HAM, the ADM, and the HPM and its exact solution are presented in Table 2.

From the Table 2, it is perceived that at each time mentioned in the table, the HAM result is better than that of the ADM and HPM. Further, the HAM has a special advantage that controls the ROC by selecting

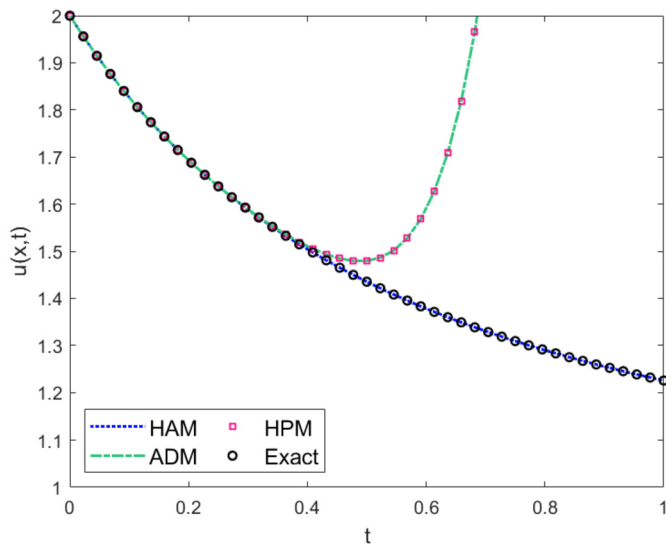


Fig. 7. A comparison between the exact solution and the approximate series solutions obtained by the HAM, the HPM, and the ADM of Eq. (9) when  $h = -0.55$  and  $\gamma = 2$  are taken.

Table 2. The AErrs of the approximate series solutions of Eq. (9) by different methods and the exact solution.

$t$	AErr when $\gamma = 2$		
	HAM	ADM	HPM
0	0	0	0
0.25	$1.13 \times 10^{-5}$	$1.09 \times 10^{-4}$	$1.09 \times 10^{-4}$
0.50	$1.81 \times 10^{-5}$	$4.43 \times 10^{-2}$	$4.43 \times 10^{-2}$
0.75	$1.34 \times 10^{-5}$	$1.41 \times 10^0$	$1.41 \times 10^0$
1.00	$5.60 \times 10^{-5}$	$1.59 \times 10^1$	$1.59 \times 10^1$

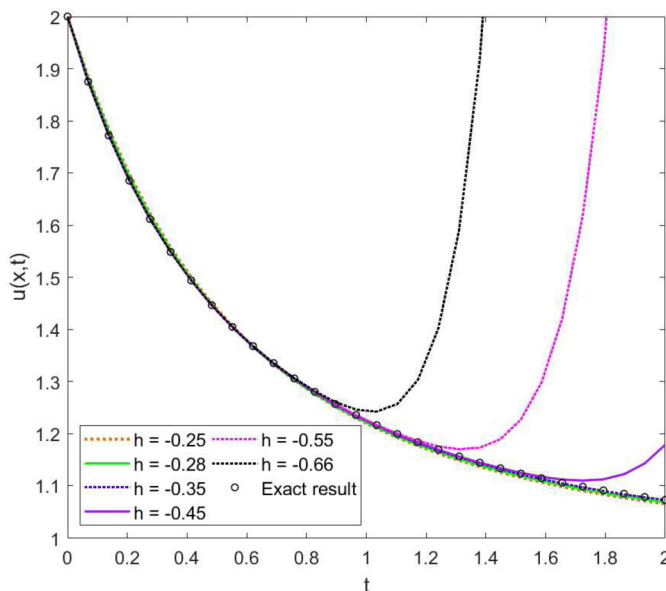


Fig. 8. A comparison between the approximate series solution of Eq. (9) given by Eq. (15) obtained by the HAM with different values of  $h$  and the exact solution of Eq. (9), where  $\gamma = 2$  is taken into account.

suitable values of the CCP  $h$ . To justify this advantage of the HAM, we exhibit the approximation series solutions of Eq. (9) given by Eq. (15) by taking the first 8 terms for several values of  $h$  in Fig. 8. It is seen from Fig. 8 that the parameter  $h$  controls the ROC. It is interesting to note here that the approximate series solution of Eq. (9) given by Eq. (15)

Table 3. The AErr and relative error of the approximate series solution of Eq. (9) and its exact solution (when  $\gamma = 2, h = -0.35$ ).

$t$	AErr	Relative error
0	0	0
0.50	$7.41 \times 10^{-4}$	$5.16 \times 10^{-4}$
1.00	$1.69 \times 10^{-3}$	$1.38 \times 10^{-3}$
1.50	$1.55 \times 10^{-3}$	$1.38 \times 10^{-3}$
2.00	$4.34 \times 10^{-4}$	$4.05 \times 10^{-4}$

by taking the first 8 terms converges to the exact solution mostly for  $h = -0.35$ . AErrs of the approximation series solution of Eq. (9) and its exact solution for varying  $t$  is presented in Table 3 with  $h = -0.35$ .

Thus, it is suggestive that the Fisher-KPP model can be used to emulate biological invasion in various affections, but it cannot be used to emulate biological recession, as the Fisher-KPP model does not allow the solution to go extinct for all cases. For removing this limitation, we need to modify the Fisher-KPP model for simulating biological recession so that the population eventually can become extinct in all cases. However, the outcomes indicate that the HAM is a powerful mathematical technique for extracting exact and analytical solutions to nonlinear equations.

### 5. Conclusion

In this paper, we have promoted the solution of the nonlinear Fisher type equations using the HAM and studied the nature of the solutions from the viewpoint of ecology and biology. It is observed that every positive IC with compact support of the Fisher's equation amplifies to a TW with a minimal speed. The effects of the proliferation rate in the Fisher-KPP model is discussed on the entire population and it is observed that the invasive cell or the invasive population decreases within a short period of time whereas the proliferation rate is minimum. The HAM includes a certain CCP that provides a convenient way to control the ROC and convergence rate of the series solution. Thus, we can extend or shorten the experimental region by controlling the CCP  $h$  when the closed form is unavailable. Also, the solutions extracted by the HAM contain the solutions obtained by the HPM and ADM. Therefore, it is confirmed that the HAM is superior to other semi-analytical methods. In the present study, Matlab software is used to figure out different effective graphs of the solution of the Fisher's equation obtained via the HAM by setting the several values of the parameter  $h$  in which Fig. 8 indicates  $h$  controls the ROC. The approximated results of Eq. (9) (Fisher's equation) by the HAM containing only first 8 terms matches reasonably well with the exact solution of the equation with respect to the RMSE value. However, our approximated outcomes are nearly identical within the range  $6 \leq N \leq 9$ . For a reasonable case,  $N = 9$  is justified, and for larger  $N$ , approximate solutions may approach the exact result. The outcomes show that the HAM is a powerful and efficient method for obtaining an analytic approximation solution to a nonlinear problem that converges to the actual solution relatively rapid (after just five iterations in the case of the current study, see Fig. 6). Since in the case of ecology or biology, the invasive species or invasion cell cannot counteract totally at any instant of time using the Fisher-KPP model, we need to reformulate the Fisher's equation. For this purpose, we deliberate that if the diffusivity  $D$  in the Fisher's equation (2) is altered, the graph of the approximate solution may be terminated after a finite number of steps even in closed-form and so the invasive species may be counteracted in a concise stage. Future scope and perspective of our research work concentrates on investigating precisely under what conditions solutions go to travelling waves or become extinct modifying the assumption that the contact point corresponds to zero cell density and on examining how quickly travelling waves develop as  $t \rightarrow \infty$ .



## Declarations

### Author contribution statement

Gour Chandra Paul: Conceived and designed the experiments; Contributed reagents, materials, analysis tools or data; Wrote the paper.

Tauhida: Performed the experiments; Analyzed and interpreted the data; Wrote the paper.

Dipankar Kumar: Conceived and designed the experiments; Wrote the paper.

### Funding statement

Tauhida was supported by Research fellowship of National Science and Technology (NST), Bangladesh [39.00.0000.012.002.05.20-05].

### Data availability statement

Data will be made available on request.

### Declaration of interests statement

The authors declare no conflict of interest.

### Additional information

No additional information is available for this paper.

## Acknowledgements

We thank the editor and three anonymous referees for invaluable comments and suggestions that helped improve and clarify this manuscript.

## References

- [1] T. Harko, M.K. Mak, Exact travelling wave solutions of non-linear reaction-convection-diffusion equations-an Abel equation-based approach, *J. Math. Phys.* 56 (11) (2015) 111501.
- [2] R.A. Fisher, The wave of advance of advantageous genes, *Ann. Eugen.* 7 (4) (1937) 355–369.
- [3] J.D. Murray, *Mathematical Biology I. An Introduction*, Springer, New York, NY, 2002.
- [4] P. Grindrod, *Patterns and Waves*, Oxford University Press, Oxford, UK, 2007.
- [5] M. El-Hachem, S.W. McCue, W. Jin, Y. Du, M.J. Simpson, Revisiting the Fisher-Kolmogorov-Petrovsky-Piskunov equation to interpret the spreading-extinction dichotomy, *Proc. R. Soc. A, Math. Phys. Eng. Sci.* 475 (2229) (2019) 20190378.
- [6] A.N. Kolmogorov, I.G. Petrovskii, N.S. Piskunov, A study of the diffusion equation with increase in the amount of substance, and its application to a biological problem, *Bull. Mosc. Univ. Math. Mech.* 1 (6) (1937) 1–25.
- [7] P.K. Maini, D.S. McElwain, D.I. Leavesley, Traveling wave model to interpret a wound-healing cell migration assay for human peritoneal mesothelial cells, *Tissue Eng.* 10 (3–4) (2004) 475–482.
- [8] P.K. Maini, D.L. McElwain, D.I. Leavesley, Traveling waves in a wound healing assay, *Appl. Math. Lett.* 17 (5) (2004) 575–580.
- [9] M.J. Simpson, K.K. Treloar, B.J. Binder, P. Haridas, K.J. Manton, D.I. Leavesley, D.S. McElwain, R.E. Baker, Quantifying the roles of cell motility and cell proliferation in a circular barrier assay, *J. R. Soc. Interface* 10 (82) (2013) 20130007.
- [10] A.M. Wazwaz, A. Gorguis, An analytic study of Fisher's equation by using Adomian decomposition method, *Appl. Math. Comput.* 154 (3) (2004) 609–620.
- [11] K.R. Swanson, C. Bridge, J.D. Murray, E.C. Alvord Jr, Virtual and real brain tumors: using mathematical modeling to quantify glioma growth and invasion, *J. Neurol. Sci.* 216 (1) (2003) 1–10.
- [12] D.J. Warne, R.E. Baker, M.J. Simpson, Using experimental data and information criteria to guide model selection for reaction-diffusion problems in mathematical biology, *Bull. Math. Biol.* 81 (6) (2019) 1760–1804.
- [13] R. Singh, D.K. Maurya, Y.K. Rajoria, A novel approach of homotopy perturbation technique to solution of non-linear Fisher equation, *Int. J. Appl. Eng. Res.* 14 (4) (2019) 957–964.
- [14] J.A. Sherratt, J.D. Murray, Models of epidermal wound healing, *Proc. R. Soc. B, Biol. Sci.* 241 (1300) (1990) 29–36.
- [15] W. Jin, E.T. Shah, C.J. Penington, S.W. McCue, L.K. Chopin, M.J. Simpson, Reproducibility of scratch assays is affected by the initial degree of confluence: experiments, modelling and model selection, *J. Theor. Biol.* 390 (2016) 136–145.
- [16] K.J. Painter, J.A. Sherratt, Modelling the movement of interacting cell populations, *J. Theor. Biol.* 225 (3) (2003) 327–339.
- [17] N. Shigesada, K. Kawasaki, Y. Takeda, Modeling stratified diffusion in biological invasions, *Am. Nat.* 146 (2) (1995) 229–251.
- [18] J. Steele, J. Adams, T. Sluckin, Modelling paleoindian dispersals, *World Archaeol.* 30 (2) (1998) 286–305.
- [19] S.A. Levin, H.C. Muller-Landau, R. Nathan, J. Chave, The ecology and evolution of seed dispersal: a theoretical perspective, *Annu. Rev. Ecol. Evol. Syst.* 34 (1) (2003) 575–604.
- [20] B.G. Sengers, C.P. Please, R.O. Oreffo, Experimental characterization and computational modelling of two-dimensional cell spreading for skeletal regeneration, *J. R. Soc. Interface* 4 (17) (2007) 1107–1117.
- [21] M. El-Hachem, S.W. McCue, M.J. Simpson, Invading and receding sharp-fronted travelling waves, *Bull. Math. Biol.* 83 (4) (2021) 1–25.
- [22] M. Shakeel, Travelling wave solution of the Fisher-Kolmogorov equation with non-linear diffusion, *Appl. Math.* 4 (8A) (2013) 148–160.
- [23] M. Matinfar, M. Ghanbari, Homotopy perturbation method for the generalized Fisher's equation, *J. Appl. Math.* 7 (2010) 39–44.
- [24] M. Matinfar, M. Ghanbari, Solving the Fisher's equation by means of variational iteration method, *Int. J. Contemp. Math. Sci.* 4 (5–8) (2009) 343–348.
- [25] O.P. Singh, R.K. Pandey, V.K. Singh, An analytic algorithm of Lane-Emden type equations arising in astrophysics using modified homotopy analysis method, *Comput. Phys. Commun.* 180 (7) (2009) 1116–1124.
- [26] S.J. Liao, The proposed homotopy analysis technique for the solution of nonlinear problems, PhD thesis, Shanghai Jiao Tong University, 1992.
- [27] S.J. Liao, Homotopy analysis method: a new analytical technique for nonlinear problems, *Commun. Nonlinear Sci. Numer. Simul.* 2 (2) (1997) 95–100.
- [28] I. Hashim, Comments on "A new algorithm for solving classical Blasius equation" by L. Wang, *Appl. Math. Comput.* 176 (2) (2006) 700–703.
- [29] A.S. Bataineh, M.S. Noorani, I. Hashim, Solving systems of ODEs by homotopy analysis method, *Commun. Nonlinear Sci. Numer. Simul.* 13 (10) (2008) 2660–2670.
- [30] S.J. Liao, A kind of approximate solution technique which does not depend upon small parameters—II. An application in fluid mechanics, *Int. J. Non-Linear Mech.* 32 (5) (1997) 815–822.
- [31] S.J. Liao, A sample approach of enlarging convergence regions of perturbation approximations, *Nonlinear Dyn.* 19 (2) (1999) 93–111.
- [32] A. Renuka, M. Muthamilselvan, D.H. Doh, G.R. Cho, Entropy analysis and nanofluid past a double stretchable spinning disk using homotopy analysis method, *Math. Comput. Simul.* 171 (C) (2020) 152–169.
- [33] S. Suharsono, S. Wulandari, A. Nuryaman, M. Usman, W. Wamiliana, J. Daoud, Solution of the reverse flow reactor model using homotopy analysis method, *IJUM Eng. J.* 22 (1) (2021) 129–137.
- [34] N.N. Hymavathi Talla, W. Sridhar, Homotopy analysis to MHD visco-elastic fluid flow and heat transfer over an exponentially stretching sheet, *Ann. Rom. Soc. Cell Biol.* 25 (3) (2021) 1850–1857.
- [35] S.J. Liao, A new analytic algorithm of Lane-Emden type equations, *Appl. Math. Comput.* 142 (1) (2003) 1–16.
- [36] S. Hasnain, M. Saqib, Numerical study of one-dimensional Fishers KPP equation with finite difference schemes, *Am. J. Comput. Math.* 7 (1) (2017) 70–83.
- [37] K. Hosseini, M. Ilie, M. Mirzazadeh, D. Baleanu, C. Park, S. Salahshour, The Caputo-Fabrizio time-fractional Sharma-Tasso-Olver-Burgers equation and its valid approximations, *Commun. Theor. Phys.* (2022).
- [38] K. Hosseini, M. Ilie, M. Mirzazadeh, A. Yusuf, T.A. Sulaiman, D. Baleanu, S. Salahshour, An effective computational method to deal with a time-fractional nonlinear water wave equation in the Caputo sense, *Math. Comput. Simul.* 187 (2021) 248–260.
- [39] K. Hosseini, K. Sadri, M. Mirzazadeh, A. Ahmadian, Y-M. Chu, S. Salahshour, Reliable methods to look for analytical and numerical solutions of a nonlinear differential equation arising in heat transfer with the conformable derivative, *Math. Methods Appl. Sci.* (2021) 1–13.
- [40] K. Hosseini, M. Ilie, M. Mirzazadeh, D. Baleanu, An analytic study on the approximate solution of a nonlinear time-fractional Cauchy reaction-diffusion equation with the Mittag-Leffler law, *Math. Methods Appl. Sci.* 44 (8) (2021) 6247–6258.